ease, G_{M1} gangliosidosis, and fucosidosis. Because this approach depends on the presence of residual enzyme activity, it would be anticipated to be most effective in juvenile, adult, and chronic forms of these diseases, rather than the infantile forms in which there is little or no residual enzyme activity. The current application of enzyme replacement to Gaucher disease is limited by the fact that the enzyme cannot cross the blood-brain barrier; hence, this therapy is only efficacious in type 1 disease where there is no neuropathology involved. NB-DNJ would not be anticipated to show efficacy in the treatment of Krabbe's disease and metachromatic leukodystrophy because both of these diseases involve the storage of galactosylceramide (GalCer)-based GSLs (GalCer and sulfatide, respectively). NB-DNJ fails to inhibit the galactosyltransferase that initiates the biosynthesis of this pathway (*17*). This is important when considering the use of this compound in humans because the formation of GalCer and sulfatide, which are both important constituents of myelin, will not be affected by NB-DNJ treatment, and therefore myelination and myelin stability should not be impaired. It will be of interest to determine which aspects of the various disease symptoms can be prevented or reversed with this approach. This will await testing of NB-DNJ in symptomatic mouse models of these diseases (*10*) and evaluation of NB-DNJ in the clinic.

REFERENCES AND NOTES

1. E. F. Neufeld, *Annu. Rev. Biochem.* **60**, 257 (1991).
2. E. Beutler, *Science* **256**, 794 (1992).
3. N. W. Barton *et al.*, *N. Engl. J. Med.* **324**, 1464 (1991).
4. E. Beutler *et al.*, *Blood* **78**, 1183 (1991).
5. F. M. Platt, G. R. Neises, R. A. Dwek, T. D. Butters, *J. Biol. Chem.* **269**, 8362 (1994); F. M. Platt, G. R. Neises, G. B. Karlsson, R. A. Dwek, T. D. Butters, *ibid.*, p. 27108.
6. F. M. Platt and T. D. Butters, *Trends Glycosci. Glycotechnol.* **7**, 495 (1995).
7. F. M. Platt, G. Reinkensmeier, R. A. Dwek, T. D. Butters, in preparation.
8. S. Yamanaka *et al.*, *Proc. Natl. Acad. Sci. U.S.A.* **91**, 9975 (1994).
9. K. Sandhoff, E. Conzelmann, E. F. Neufeld, M. M. Kaback, K. Suzuki, in *The Metabolic Basis of Inherited Disease*, C. R. Scriver, A. L. Beaudet, W. S. Sly, D. Valle, Eds. (McGraw-Hill, New York, 1989), vol. 2, pp. 1807–1839.
10. K. Sango *et al.*, *Nature Genet.* **11**, 170 (1995).
11. M. Taniike *et al.*, *Acta Neuropathol.* **89**, 296 (1995).
12. From weaning (4 weeks), mice were fed a diet of powdered mouse chow (expanded Rat and Mouse Chow 1, ground, SDS Ltd., Witham, Essex, UK) containing NB-DNJ. The diet and compound (both dry solids) were mixed thoroughly before use, stored at room temperature, and used within 7 days of mixing. Water was available to the mice ad libitum. The mice were housed under standard nonsterile conditions and were given 4800 mg per kilogram of body weight per day of NB-DNJ, which gave serum concentrations of ~50 μM (data not shown).
13. M. A. Fischl *et al.*, *J. Acquired Immune Defic. Syndr.* **7**, 139 (1994).
14. The animals were anesthetized, perfused with phosphate-buffered saline (PBS) (pH 7.2), and the intact brain removed. The brain tissue was manually homogenized in water, freeze-dried, and extracted twice with chloroform:methanol 2:1 (v/v) for 2 hours at room temperature and overnight at 4°C. A volume of the solvent extract equivalent to 5 mg dry weight for each brain was base hydrolyzed (*10*), and the Folch upper phase was separated by TLC (Silica gel 60 plates, Merck, British drug house, Poole, Dorset, UK) in chloroform:methanol: 0.22% calcium chloride (60:35:8), then sprayed with orcinol and visualized by heating to 80°C for 10 min.
15. Mice were anesthetized, perfused with PBS (pH 7.4) containing 4% paraformaldehyde, and the brain dissected and retained in fixative overnight prior to cryopreservation and sectioning. Frozen brain sections (7 μm) were warmed to room temperature, stained with PAS according to the manufacturer's instructions (Sigma, Poole, Dorset, UK), counterstained with Erhlich's hematoxylin, and mounted in diethyl-(phenyl)xanthine (British drug house).
16. The mice were anesthetized and perfusion fixed with 2% paraformaldehyde, 2% glutaraldehyde mix in PBS. The brain was dissected and fixed in the same fixative overnight at 4°C. The brain was trimmed, and 100-μm sections were cut on a vibrotome, then washed three times in 0.1 M phosphate buffer and stained with osmium tetroxide (1% in 0.1 M phosphate) for 35 min. The sections were dehydrated through an ethanol series, treated with propylene oxide (twice for 15 min), and then placed in Durcupan resin overnight at room temperature, transferred to glass slides, and kept at 60°C for 48 hours. Storage areas of the brain were selected microscopically, cut out of the thick section with a scalpel blade, and transferred to propylene oxide and embedded in Embed 800 (Electron Microscopy Sciences, Fort Washington, PA). Sections were stained with uranyl acetate/lead citrate and observed with a Hitachi 600 microscope at 75 kV.
17. T. Butters, unpublished observation.
18. F. Platt, unpublished observation.

19. We thank Searle/Monsanto for NB-DNJ, J. Vass and D. Smith for excellent technical assistance, and C. Beesley for photography. The Glycobiology Institute is supported by Searle/Monsanto. F.M.P. is a Lister Institute Research Fellow.

26 December 1996; accepted 28 February 1997

Crystal Structure of the Nucleotide Exchange Factor GrpE Bound to the ATPase Domain of the Molecular Chaperone DnaK

Celia J. Harrison, Manajit Hayer-Hartl, Maurizio Di Liberto, F.-Ulrich Hartl, John Kuriyan*

The crystal structure of the adenine nucleotide exchange factor GrpE in complex with the adenosine triphosphatase (ATPase) domain of *Escherichia coli* DnaK [heat shock protein 70 (Hsp70)] was determined at 2.8 angstrom resolution. A dimer of GrpE binds asymmetrically to a single molecule of DnaK. The structure of the nucleotide-free ATPase domain in complex with GrpE resembles closely that of the nucleotide-bound mammalian Hsp70 homolog, except for an outward rotation of one of the subdomains of the protein. This conformational change is not consistent with tight nucleotide binding. Two long α helices extend away from the GrpE dimer and suggest a role for GrpE in peptide release from DnaK.

Molecular chaperones play an essential role in protein folding by preventing the misfolding and aggregation of folding intermediates (*1–3*). Several classes of molecular chaperones have been conserved in evolution, including the members of the Hsp70, Hsp90, and Hsp60 (chaperonin) families. Whereas the chaperonins form large oligomeric ring structures, members of the Hsp70 and Hsp90 families function as monomers or dimers.

DnaK, the *Escherichia coli* homolog of Hsp70, and the various eukaryotic Hsp70s act by binding and releasing extended peptide segments enriched in hydrophobic side chains. DnaK and its homologs are composed of an NH_2-terminal 42-kD ATPase domain and a COOH-terminal 25-kD peptide binding domain, the structures of which are known (*4*, *5*). The binding and release of peptides from DnaK is controlled by conformational changes induced by adenosine triphosphate (ATP) binding and hydrolysis in a mechanism that is not understood. In this reaction DnaK does not act alone but cooperates with two other factors, the chaperone DnaJ and the nucleotide exchange factor GrpE (*6*), in a manner that is analogous to the regulation of many guanosine triphosphate binding proteins.

The following model of the DnaK reaction cycle in protein folding is now emerging (*7*): ATP-bound DnaK is characterized by rapid peptide binding and release (*8*). DnaJ stimulates the hydrolysis of ATP by

C. J. Harrison and J. Kuriyan, Laboratories of Molecular Biophysics and Howard Hughes Medical Institute, Rockefeller University, 1230 York Avenue, New York, NY 10021, USA.
M. Hayer-Hartl, M. Di Liberto, F.-U. Hartl, Cellular Biochemistry and Biophysics Program, Howard Hughes Medical Institute, and Memorial Sloan-Kettering Cancer Center, 1275 York Avenue New York, NY 10021, USA. After 15 June 1997, these authors will be at Max-Planck-Institute for Biochemistry, Am Klopferspitz 18A, 82152 Martinsried, Germany.

*To whom correspondence should be addressed.

DnaK, resulting in the adenosine diphosphate (ADP)–bound state of DnaK, which binds peptide tightly (6, 7). Peptide release then requires the dissociation of ADP, which is catalyzed by GrpE, and ATP rebinding to DnaK then occurs (8, 9). Interestingly, whereas the function of DnaK and of mitochondrial Hsp70 critically depends on GrpE, the Hsp70 homologs in the eukaryotic cytosol are GrpE-independent (10–12). For these Hsp70s, ADP dissociation is apparently not a rate-limiting step in the reaction cycle.

We now describe the three-dimensional structure of the ATPase domain of *E. coli* DnaK in complex with GrpE. In addition to providing a structural explanation for the ability of GrpE to release nucleotide from DnaK, a striking architectural feature of the structure suggests a role for GrpE in influencing DnaK-peptide interactions.

The *E. coli* DnaK ATPase domain (residues 1 to 388) and full-length *E. coli* GrpE (residues 1 to 197) were overexpressed in *E. coli*. A mutant form of GrpE (G122D, in which Gly at position 122 is mutated to Asp) was used. The mutant confers a temperature-sensitive growth phenotype but is fully functional in mediating DnaK-DnaJ–assisted protein folding in vitro (13). Dimeric GrpE was digested with elastase, with loss of the NH_2-terminal 33 residues, and a ~164-residue proteolytic fragment was purified to homogeneity. Identical proteolysis results were seen in the presence and absence of the DnaK ATPase domain. A stable complex between one DnaK ATPase domain and a dimer of truncated GrpE was formed in the absence of ATP, purified, and crystallized (14).

Native crystals diffract weakly, to ~3.5 Å on a rotating anode x-ray generator. Crystals derivatized with uranyl acetate diffracted better than native crystals; a single crystal derivatized with uranyl acetate was used for the final refinement after the structure solution by multiple isomorphous replacement (MIR) (Table 1). The final model has been refined at 2.8 Å [*R* value of 0.223 ($F > 2\sigma$) and R_{free} of 0.317 ($F > 2\sigma$)]. The final model contains a dimer of GrpE and one DnaK ATPase domain in the asymmetric unit.

GrpE is a tightly associated homodimer that binds DnaK with 2:1 stoichiometry (15, 16). The overall identity between GrpE sequences ranges from 25 to 70%, and the conservation of buried side chains suggests that the structure (Fig. 1) is likely to be conserved. The GrpE dimer interface encompasses two long, paired α helices that lead into a small four-helix bundle to which each monomer contributes two helices (Fig. 2A). The two long helices and the four-helix bundle bury 2600 and 2100 Å^2 of total solvent-accessible surface area, respectively, calculated with a probe radius of 1.4 Å. The loop connecting the long and short α helices is partially disordered in one of the GrpE monomers and totally disordered in the other. On the basis of weak electron density for one monomer, we favor a model without crossover of protein chains at the base of the four-helix bundle.

Whereas the topology of the polypeptide fold is similar in each monomer, the structure of the dimer is strikingly asymmetric, with the GrpE dimer being curved toward DnaK. The two long helices in the dimer do not form a canonical coiled-coil but instead lie nearly in the same plane and are translated slightly with respect to each other along the helix axis. The canonical i+3, i+4 heptad repeat of hydrophobic residues is not adhered to in GrpE. Instead there are two missteps [or stutters (17)] in the heptad repeat (i+3, i+4, i+3, i+4, i+4, i+3, i+4, i+3, i+4, i+4) that cause overwinding of the helices in some regions and a loss of superhelicity.

The GrpE monomer proximal to DnaK contributes the bulk of the residues at the DnaK interface. Starting at the NH_2-termini of the long helices, the helix of the distal monomer continues unbroken for 19 turns, that is, ~100 Å. In contrast, the helix of the proximal GrpE loses helicity between Phe^{86} and Leu^{88}. Helicity of the proximal long helix is resumed at the start of the four-helix bundle. Two small β sheet domains emanate from the two COOH-terminal ends of the four-helix bundle of GrpE. The compact β domains are ~60 residues in length, have six short β strands, and a limited hydrophobic core.

The ATPase domain actually consists of two large domains, each of which is composed of two subdomains (4). Subdomains IA and IIA, which lie at the base of the deep nucleotide binding cleft, are similar in topology and are related by pseudo twofold symmetry. Subdomains IB and IIB, which make up the sides of the nucleotide binding site, represent insertions in IA and IIA, respectively, and are not topologically related.

The ATPase domain from bovine brain heat shock cognate 70 (Hsc70) is 55% identical in sequence to that of DnaK. Insertions and deletions in DnaK relative to Hsc70 are all accommodated in surface-exposed loops (DnaK residues 43 to 47, 105 to 111, and 288 to 291), and none of these results in a changed topology or has any obvious consequence for GrpE interaction. We compared the structure of GrpE-bound, nucleotide-free DnaK with that of nucleotide-bound Hsc70. The

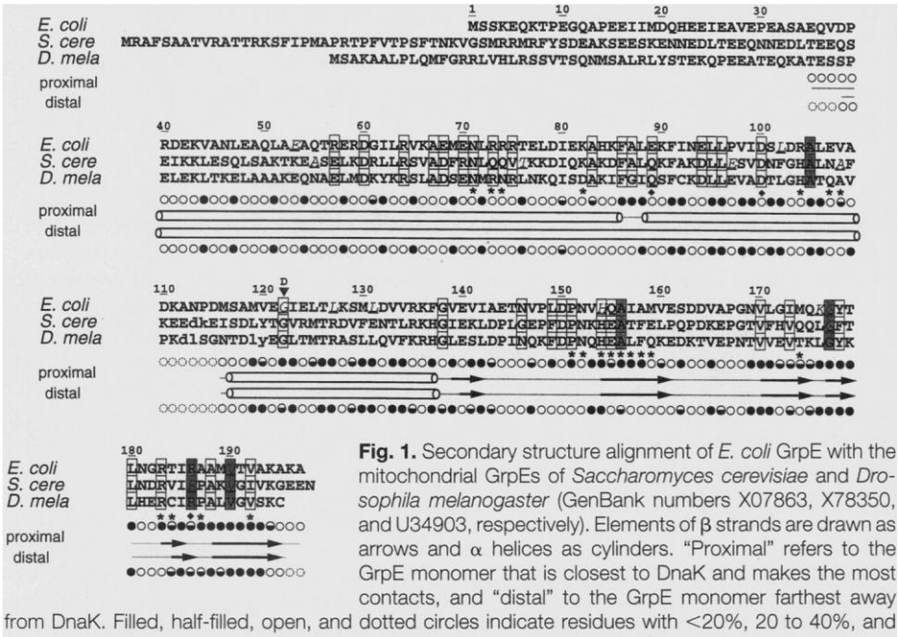

Fig. 1. Secondary structure alignment of *E. coli* GrpE with the mitochondrial GrpEs of *Saccharomyces cerevisiae* and *Drosophila melanogaster* (GenBank numbers X07863, X78350, and U34903, respectively). Elements of β strands are drawn as arrows and α helices as cylinders. "Proximal" refers to the GrpE monomer that is closest to DnaK and makes the most contacts, and "distal" to the GrpE monomer farthest away from DnaK. Filled, half-filled, open, and dotted circles indicate residues with <20%, 20 to 40%, and >40% solvent-accessible surfaces and residues that were not modeled, respectively. Invariant residues in 20 GrpE sequences in the database (31) are shaded; some of the highly conserved residues are boxed; residues that contact DnaK have an asterisk; and invariant or highly conserved residues involved in intramolecular contacts have a diamond. Known mutations of GrpE or yeast mitochondrial homolog Mge1p are shown italicized and underlined (19–21). The G122D mutant used in this study is indicated. Lower-case letters indicate insertions (not shown) in a sequence relative to *E. coli*. Abbreviations for the amino acid residues are as follows: A, Ala; C, Cys; D, Asp; E, Glu; F, Phe; G, Gly; H, His; I, Ile; K, Lys; L, Leu; M, Met; N, Asn; P, Pro; Q, Gln; R, Arg; S, Ser; T, Thr; V, Val; W, Trp; and Y, Tyr.

close similarity in the structures of the nucleotide-bound forms of Hsc70 and actin (*4*), which share only ~10% sequence identity, suggests that the structure of Hsc70 is a good model for the much more closely related DnaK.

GrpE induces a 14° rotation of domain IIB in DnaK relative to its position in the Hsc70 structure. In spite of this marked rotation, domain IIB itself is quite similar to the equivalent domain in the Hsc70 homolog [0.8 Å root-mean-square deviation (rmsd) for 79 Cα positions after superimposition]. The remainder of DnaK superimposes very well with Hsc70 and shows negligible changes because of GrpE binding (0.7 Å rmsd for 216 equivalent Cα positions) (Fig. 2B).

There are six areas of contact between DnaK and GrpE (Fig. 2C). The two largest are between the two faces of the proximal β sheet domain of GrpE and domains IB and IIB of DnaK, on each side of the nucleotide binding cleft. The other areas are on separate regions of the GrpE long helix, on either side of the β sheet domain. The interface includes nonpolar, polar, and salt bridge interactions. The total solvent-accessible surface area contributed by GrpE and DnaK to the interface is about 2800 Å^2, a typical value for tight protein-protein interactions (*18*). Most of the known mutations in GrpE that confer temperature-sensitive phenotypes (*19–21*) appear to be involved in structural stabilization and not in interactions with DnaK (Fig. 1).

The asymmetry in the structure of the GrpE dimer explains the 1:2 stoichiometry of the complex that is observed biochemically (*15*, *16*). The binding of a second ATPase domain to the distal β sheet domain of GrpE would result in a deformation of our GrpE structure. Although not directly involved in DnaK interactions, Phe^{86} (proximal GrpE) is used to properly position the β sheet domain side chain Arg^{183}, which forms an intermolecular hydrogen bond with Glu^{28} of DnaK. Phe^{86} (distal GrpE) would not be able to pack against the aliphatic portion of the Arg^{183} side chain of GrpE without the local distortion of the long helix that is seen in the proximal GrpE monomer. The four-helix bundle also bends toward the DnaK ATPase domain to optimize an area of GrpE-DnaK interaction (Fig. 2C).

The GrpE-DnaK complex is free of nucleotide, whereas in the structure of the ATPase domain of bovine brain Hsc70, ADP is buried and tightly bound in the interdomain cleft. The GrpE-induced movement of domain IIB displaces by 2 to 3 Å three residues in DnaK that hydrogen bond to the adenine and ribose rings of ADP in Hsc70. These are Ser^{274}, Lys^{270}, and Glu^{267}, which are equivalent to Ser^{275}, Lys^{271}, and Glu^{268} in bovine Hsc70 (Fig. 3). The nucleotide binding site is thus disrupted in the GrpE-DnaK complex by the mechanical opening of the DnaK structure, with GrpE itself remaining distant from the nucleotide binding site.

We used surface plasmon resonance to determine the apparent association and dissociation rates for the complex of full-length GrpE and full-length DnaK (*22*). In the absence of nucleotide, the complex forms with an on-rate of ~5×10^4 M^{-1} s^{-1} and dissociates with a half-time ($t_{1/2}$) of ~10 min, resulting in an apparent dissociation constant (K_d) of ~30 nM. In the presence of ADP, the on-rate for DnaK binding was reduced ~20-fold, whereas ADP had little effect on the dissociation of the complex. In contrast, no complex formation was detected in the presence of ATP. Addition of ATP to a nucleotide-free complex caused instantaneous dissociation. We conclude that GrpE recognizes the ADP-bound state of DnaK and results in ADP dissociation.

At present, the only other structure of a nucleotide exchange factor in complex with its nucleotide binding protein is that of the *E. coli* elongation factor EfTu, a GTP binding protein, in complex with the exchange

Table 1. Crystals ($P4_1$, $a = b = 150.3$ Å, $c = 49.1$ Å, $\alpha = \beta = \gamma = 90°$) were grown by vapor diffusion of complex (40 mg/ml) and 3.5% PEG 8000, 15% ethylene glycol, 50 mM sodium acetate buffer (pH 4.6), 190 mM lithium sulfate, 5 to 10 mM dithiothreitol, and 10 mM (D,L)-methionine in a nitrogen atmosphere at 4°C. Data were collected at 100 K on an Raxis IIC (Rigaku) and indexed, integrated, and scaled with the DENZO package (*26*). On the basis of a preliminary model, three residues in DnaK (Arg^{235}, Asp^{289}, and Asp^{385}) were mutated to cysteine. Derivatization of isomorphous crystals with ethyl-mercury phosphate (EMP) resulted in heavy atom substitution at each of the new cysteine sites as well as the native Cys^{17} for R235C and D289C DnaK. MIR phases were calculated to 3.6 Å with MLPHARE (13,042 reflections, figure of merit, 0.56) and solvent flattened with DPHASES in the GVX program suite (*27*). The model was built into the electron density maps by using O (*28*) and MAIN (*29*). The model was refined with X-PLOR (*30*). Experimentally determined seleno-methionine peaks confirmed the topology of the GrpE molecule (*14*). The final model includes residues 3 to 383 of DnaK (except residues 184 and 210 to 213, which are disordered) and residues 34 to 197 (except residues 108 to 115) for the GrpE monomer that is proximal to DnaK in the complex, and residues 38 to 195 (except residues 108 to 115) for the GrpE monomer that is distal to DnaK, 28 water molecules, and 8 uranyl acetate ions, modeled as single sites. The average *B* factor for the protein model is 54 Å^2, the *B* factor estimated from the Wilson plot is 59 Å^2, and the average *B* factor for the waters is 42.5 Å^2; n/a, not applicable.

Data set	Resolution (Å)	Sites (no.)	Observations		R_{sym}*		Completeness		R_{iso}†	Phasing power‡
			Total	Unique	Total	Outer shell	Total	Outer shell		
Native I	3.6		106,989	13,050	0.081	0.246	0.963	0.801		
Seleno-Met	3.7	13 (of 22)	83,472	11,668	0.069	0.276	0.941	0.907	0.142	1.02
K_2IrCl_6	4.3	2	48,547	7,742	0.071	0.132	0.937	0.966	0.146	1.28
EMP(D289C)	3.2	2	112,874	17,520	0.087	0.282	0.949	0.872	0.190	1.44
EMP(R235C)	3.3	2	119,916	15,134	0.069	0.353	0.902	0.744	0.192	1.20
Uranyl acetate I	3.1	4 (of 7)	362,075	19,609	0.082	0.326	0.962	0.789	0.234	1.10
Uranyl acetate II	2.8	8	754,420	26,024	0.093	0.179	0.957	0.864	n/a	n/a

Refinement statistics

Data set used for native	Resolution (Å)	Reflections $F > 2\sigma$	Total atoms (no.)	R value§ (R_{free})	rmsd from ideal values		rmsd for *B* values
					Bonds	Angles	
Uranyl acetate II	30.0–2.8	23,930	5,190	0.223 (0.317)	0.012 Å	1.58°	1.52 Å^2

*$R_{sym} = \Sigma|I - \langle I\rangle|/\Sigma I$, where I is the integrated intensity of a given reflection. †$R_{iso} = \Sigma|F_{PH} - F_P|/\Sigma F_P$, where F_{PH} and F_P are the derivative and native structure factor amplitudes, respectively. ‡Phasing power = $\{\Sigma|F_{PH(calc)}|^2/\Sigma|F_{PH(obs)} - F_{P(calc)}|^2\}^{1/2}$. §$R_{value} = \Sigma|F_P - F_{p(calc)}|/\Sigma F_p$. R_{free} is the R_{value} for a subset of 8% of the reflection data that were not included in the crystallographic refinement.

factor EfTs (*23*). Like GrpE, EfTs induces a conformational change by binding to EfTu and displaces secondary structure elements necessary for competent binding of the nucleotide. Unlike GrpE, which destabilizes the binding of the purine and ribose rings, EfTs acts by destabilizing the interactions of the phosphate groups of the nucleotide. EfTs also directly competes for the binding site of the divalent cation found adjacent to the nucleotide binding site. In contrast, the nearest approach of any side chain of GrpE to the nucleotide binding site is about 13 Å.

The asymmetry of the GrpE-DnaK interaction raises an intriguing question: Why is GrpE a functional dimer? Essentially all the interactions between GrpE and the ATPase domain of DnaK involve just the proximal GrpE monomer. A major reason for dimer formation would appear to be the need to stabilize the unusually long parallel α-helical structure. However, the long helices are only minimally involved in interactions with the ATPase domain.

The elongated structure of GrpE suggests that GrpE might interact with the peptide binding domain of DnaK. The COOH-terminus of the ATPase domain is positioned such that the COOH-terminal peptide binding domain of DnaK might be located in proximity to the NH_2-terminal portion of the long helices of GrpE. A mutation at Glu^{53} of GrpE results in a temperature-sensitive phenotype for λ replication (*19*) (Fig. 3, right panel), and this residue in the long helix is located at least 22 Å from the ATPase domain and is not involved in interhelical stabilization. This suggests that the NH_2-terminal portions of the long helices of GrpE are functionally important.

To further test this possibility we analyzed the effect of GrpE on substrate binding by DnaK. We found that binding of full-length GrpE to full-length DnaK causes the dissociation of a complex between DnaK and carboxymethylated α-lactalbumin (RCMLA), a permanently unfolded model substrate of DnaK (*24*, *25*) (Fig. 4). Significantly, this dissociation was not observed with GrpE lacking residues 1 to 33, indicating

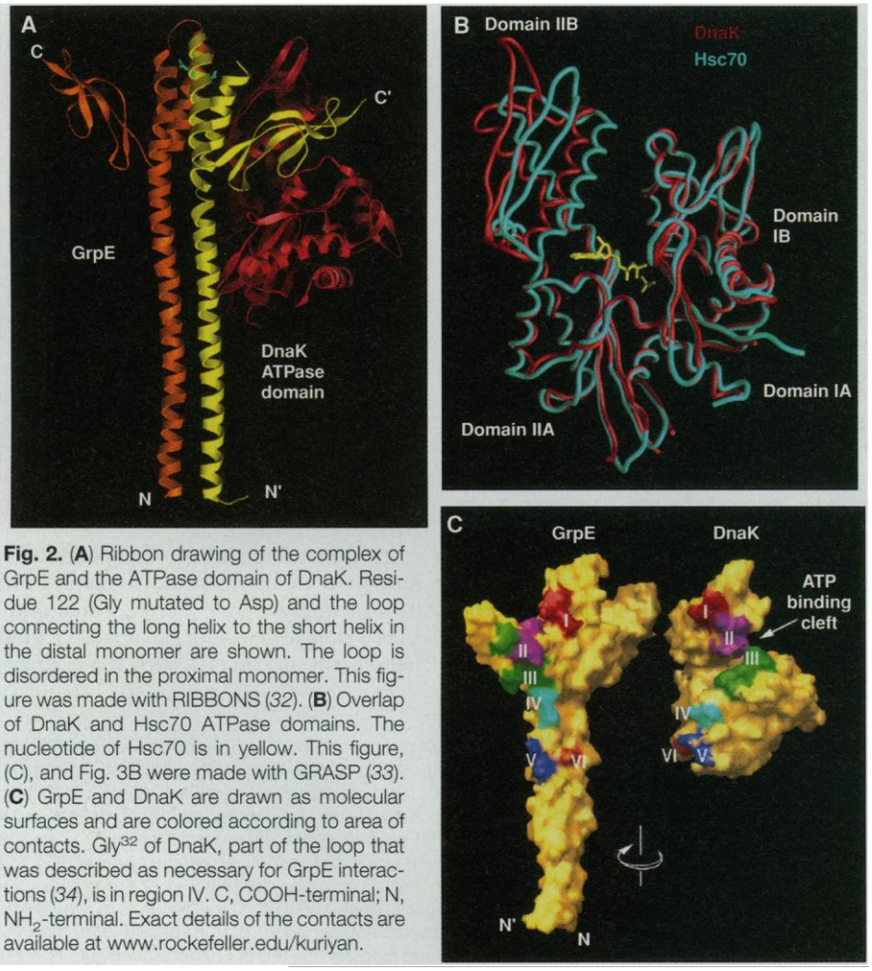

Fig. 2. (**A**) Ribbon drawing of the complex of GrpE and the ATPase domain of DnaK. Residue 122 (Gly mutated to Asp) and the loop connecting the long helix to the short helix in the distal monomer are shown. The loop is disordered in the proximal monomer. This figure was made with RIBBONS (*32*). (**B**) Overlap of DnaK and Hsc70 ATPase domains. The nucleotide of Hsc70 is in yellow. This figure, (C), and Fig. 3B were made with GRASP (*33*). (**C**) GrpE and DnaK are drawn as molecular surfaces and are colored according to area of contacts. Gly^{32} of DnaK, part of the loop that was described as necessary for GrpE interactions (*34*), is in region IV. C, COOH-terminal; N, NH_2-terminal. Exact details of the contacts are available at www.rockefeller.edu/kuriyan.

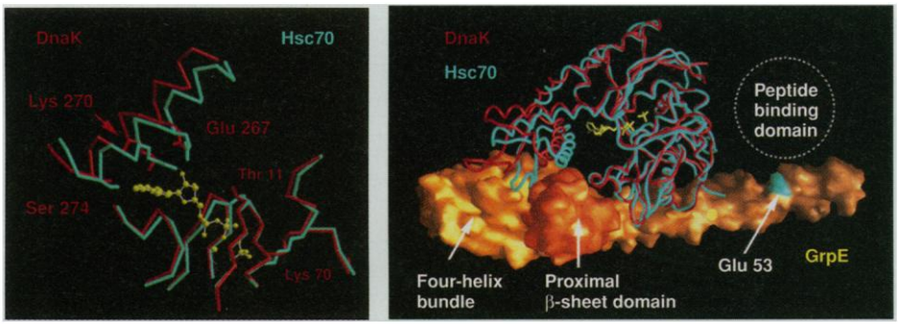

Fig. 3. Superimposition of the nucleotide binding cleft of DnaK onto bovine brain Hsc70. (**Left**) Diagram of a close-up of the nucleotide binding pocket, with DnaK (red) and Hsc70 (cyan) and Hsc70's ADP, Mg^{2+}, and inorganic phosphate (yellow). Ser^{274}, Lys^{270}, and Glu^{267} are shown to illustrate their displacement from the purine and ribose rings. (**Right**) To show the displacement of domain IIB of DnaK as a result of GrpE binding, GrpE is drawn as a molecular surface (yellow), with Hsc70 and the Hsc70 nucleotide superimposed onto the DnaK ATPase domain as described in the text. The temperature-sensitive point mutation for λ replication, Glu^{53} to Gly (*19*), is indicated with a cyan surface coloring. The COOH-terminus of the ATPase domain is directed toward the proposed location of the peptide binding domain.

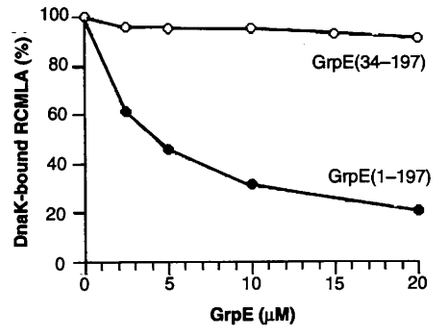

Fig. 4. Effect of GrpE binding on the interaction between DnaK and unfolded polypeptide substrate. DnaK (9 μM) was incubated for 15 min at 25°C with 9 μM ^{3}H-labeled, reduced, and carboxymethylated bovine α-lactalbumin (RCMLA) (*35*) in buffer A containing 0.005% Tween 20. Then 0 to 20 μM GrpE (closed circles) or GrpE(34–197) (open circles) was added for 15 min and the reactions analyzed by native polyacrylamide gel electrophoresis on 3 to 10% polyacrylamide gradient gels (*36*). Amounts of DnaK-bound RCMLA were quantified by densitometry.

that this presumably flexible segment is necessary for the effect. Consistent with this observation, it had previously been noted that addition of GrpE to a preformed complex of unfolded luciferase, DnaK-ADP, and DnaJ caused the dissociation of at least a fraction of luciferase from its bound chaperones (*7*). The significance of the peptide-dissociating effect of GrpE remains to be established, because the NH_2 terminally truncated form of GrpE was functional in the luciferase refolding assay (*13*). It is possible that this function of GrpE is necessary for the efficient release of certain tightly binding peptide substrates of DnaK. On the basis of the finding that the NH_2-terminal portion of GrpE facilitates peptide release, we propose that GrpE interacts with the peptide binding domain.

The mechanism of nucleotide exchange by GrpE is particularly straightforward and involves a simple opening of the nucleotide binding cleft of DnaK. This mechanism is distinct from that observed in the EFTu-EFTs case, indicating that nucleotide exchange factors have evolved independent modes of action. The unusual structure of GrpE in which two long α helices extend beyond the ATPase domain, as well as the biochemical results presented here, expands the current view of GrpE function to include a role in peptide release. This dual function of GrpE was not previously anticipated.

REFERENCES AND NOTES

1. E. A. Craig, B. D. Gambill, R. J. Nelson, *Microbiol. Rev.* **57**, 402 (1993).
2. F. U. Hartl, *Nature* **381**, 571 (1996).
3. C. Georgopoulos and W. J. Welch, *Annu. Rev. Cell Biol.* **9**, 601 (1993).
4. K. M. Flaherty, C. DeLuca-Flaherty, D. B. McKay, *Nature* **346**, 623 (1990).
5. X. Zhu *et al.*, *Science* **272**, 1606 (1996).
6. K. Liberek, J. Marszalek, D. Ang, C. Georgopoulos, M. Zylicz, *Proc. Natl. Acad. Sci. U.S.A.* **88**, 2874 (1991).
7. A. Szabo *et al.*, *ibid.* **91**, 10345 (1994).
8. D. Schmid, A. Baici, H. Gehrig, P. Christen, *Science* **263**, 971 (1994).
9. D. R. Palleros, K. L. Reid, L. Shi, W. J. Welch, A. L. Fink, *Nature* **365**, 664 (1993).
10. R. A. Stuart, D. M. Cyr, E. A. Craig, W. Neupert, *Trends Biochem. Sci.* **19**, 87 (1994).
11. J. Hohfeld, Y. Minami, F. U. Hartl, *Cell* **83**, 589 (1995).
12. T. Ziegelhoffer, P. Lopez-Bueasa, E. A. Craig, *J. Biol. Chem.* **270**, 10412 (1995).
13. Refolding of denatured firefly luciferase was as described (*7*). Final concentrations in the refolding assay were as follows: 0.1 μM luciferase, 5 μM DnaK, 1 μM DnaJ, 0 to 10 μM GrpE, and 1 mM ATP. Optimal reactivation in the presence of GrpE was 60 to 70% and 10% in the absence of GrpE (measured after incubation for 60 min at 25°C). The crystallized GrpE, truncated at the NH_2-terminus [GrpE(34–197)], was as active as full-length GrpE.
14. Purified ATPase domain of DnaK and truncated GrpE were mixed such that there was a twofold excess of DnaK relative to the GrpE dimer. About 40 mg of complex was purified away from the excess DnaK on a Sephacryl S-100 column (2.5 cm by 63 cm) in 25 mM Mopso (pH 6.8), 25 mM NaCl, 5 mM dithiothreitol, and 10 mM (D,L)-methionine. The complex was concentrated to 200 mg/ml. Seleno-methionine–substituted DnaK and GrpE complexes, as well as complexes made with the DnaK cysteine mutants R235C and D289C (R, Arg; C, Cys; D, Asp), were prepared in the same way.
15. H. J. Schonfeld, D. Schmidt, H. Shroder, B. Bukau, *J. Biol. Chem.* **270**, 2183 (1995).
16. B. Wu, A. Wawrzynov, M. Zylicz, C. Georgopoulos, *EMBO J.* **15**, 4806 (1996).
17. A. Lupas, *Trends Biochem. Sci.* **21**, 379 (1996).
18. J. Janin, *Biochimie* **77**, 497 (1995).
19. B. Wu, D. Ang, M. Snavely, C. Georgopolous, *J. Bacteriol.* **176**, 6965 (1994).
20. S. Laloraya, P. J. T. Dekker, W. Voos, E. A. Craig, N. Pfanner, *Mol. Cell. Biol.* **15**, 7098 (1995).
21. B. Westermann, C. Prip-Buus, W. Neupert, E. Schwarz, *EMBO J.* **14**, 3452 (1995).
22. Apparent association and dissociation rate constants for the interaction between DnaK and GrpE were determined from a series of surface plasmon resonance (SPR) measurements at different ligand concentrations [M. K. Hayer-Hartl, J. Martin, F. U. Hartl, *Science* **269**, 836 (1995)]. Complex formation occurred at a rate of $\sim 5 \times 10^4\ M^{-1}\ s^{-1}$ (absence of nucleotide) and $\sim 2 \times 10^3\ M^{-1}\ s^{-1}$ (with ADP), and was not measurable in the presence of ATP. The complex dissociated at the following apparent rates: $\sim 1.5 \times 10^{-3}\ s^{-1}$ (no nucleotide), $\sim 7 \times 10^{-3}\ s^{-1}$ (with ADP) and $\sim 10^{-1}\ s^{-1}$ with ATP (too fast to be determined exactly). SPR experiments were performed with a BIAcore 2000 apparatus (Pharmacia Biosensor). The carboxylated dextran matrix of the 60-nl flow cell (M5 research grade) was first activated with 1-ethyl-3-(3-dimethylaminopropyl)carbodiimide and *N*-hydroxysuccinimide to allow the subsequent cross-linking of *N*-(5-amino-1-carboxypentyl)-iminodiacetic acid (NTA) (20 mg/ml in 50 mM borate buffer, pH 8.5). After cross-linking, the reactive groups were blocked by injection of 1 M ethanolamine (pH 8.5). To activate the NTA surface, we injected $NiCl_2$ (25 mM in 10 mM tris, pH 8.0) for 6 min at 5 μl/min. Then His_6-tagged GrpE was injected at 4.5 μM in running buffer. Bound His_6-GrpE was lost from the Ni^{2+}-NTA matrix at a slow drift rate, which was taken into account in the calculation of apparent association and dissociation rates. More than 50% of the immobilized GrpE was competent in binding DnaK.
23. T. Kawashima, C. Berthet-Colominas, M. Wulff, S. Cusack, R. Leberman, *Nature* **379**, 511 (1996).
24. T. Langer *et al.*, *ibid.* **356**, 683 (1992).
25. D. R. Palleros, W. J. Welch, A. L. Fink, *Proc. Natl. Acad. Sci. U.S.A.* **88**, 5719 (1991).
26. W. Minor and Z. Otwinowski, unpublished programs.
27. G. van Duyne, unpublished programs.
28. T. A. Jones, J. Y. Zou, S. W. Cowan, M. Kjeldgaard, *Acta Crystallogr.* **A47**, 110 (1991).
29. D. Turk, unpublished programs.
30. L. M. Rice and A. T. Brunger, *Proteins* **19**, 277 (1994); J. S. Jiang and A. T. Brunger, *J. Mol. Biol.* **243**, 100 (1994).
31. D. J. Naylor, N. J. Hoogenrad, P. B. Hoj, *FEBS Lett.* **396**, 181 (1996).
32. M. Carson and C. E. Bugg, *J. Mol. Graphics* **4**, 121 (1986).
33. A. Nicholls, K. A. Sharp, B. J. Honig, *Proteins Struct. Funct. Genet.* **11**, 281 (1991).
34. A. Buchberger, H. Schroder, M. Buttner, A. Valencia, B. Bukau, *Nature Struct. Biol.* **1**, 95 (1994).
35. M. K. Hayer-Hartl, J. J. Ewbank, T. E. Creighton, F. U. Hartl, *EMBO J.* **13**, 3192 (1994).
36. T. Langer, G. Pfeifer, J. Martin, W. Baumeister, F. U. Hartl, *ibid.* **11**, 4757 (1992).

37. We thank A. Szabo for the initial clone of the ATPase domain of DnaK, S. Jacques for technical assistance, F. Sicheri and D. Jeruzalmi for help with data collection, A. Bohm for critically reading the manuscript, and H. Nelson, T. Alber, and his group for helpful discussions. The 2.8 Å data set was measured at the Cornell High Energy Synchrotron Source. The coordinates have been deposited in the Brookhaven Protein Data Bank with the accession code 1DKG.

27 November 1996; accepted 26 February 1997